Int. J. Electrochem. Sci., 8 **(2013)** 6118 - 6130

International Journal of
ELECTROCHEMICAL
SCIENCE
www.electrochemsci.org

Determination of Cefoperazone Based on Nano-Composite Electrode Using Coulometric FFT Admittance Voltammetry

Parviz Norouzi[1,2,*], *Bagher Larijani*,[2,*] *Farnoush Faridbod*,[1,2] *Mohammad Reza Ganjali*[1,2]

[1]Center of Excellence in Electrochemistry, University of Tehran, Tehran, Iran
[2]Endocrinology & Metabolism Research Center, Tehran University of Medical Sciences, Tehran, Iran
[*]E-mail: norouzi@khayam.ut.ac.ir, emrc@tums.ac.ir

Received: 30 January 2013 / *Accepted:* 26 February 2013 / *Published:* 1 May 2013

In this work, new nano-composite modified carbon paste electrode for Cefoperazone detection is presented. Nano-composite paste was made by mixing ionic liquid, 1-butyl-3-methylimidazolium hexafluorophosphate ($BMIMPF_6$), grapheme nanosheets, Au and CeO_2 nanoparticles as electrochemical mediators. The developed electrochemical method for determination of Cefoperazone was based on coulometric fast Fourier transformation admittance voltammetry (CFFTAV). The analyte signal was based on the charge under the admittance peak, which was calculated by integrating signal in a specific potential range. The response of the unmodified carbon paste electrode (CPE) was determined and compared to the modified one (MCPE). Once established the best operative optimum conditions, the resulting nano-composite electrode showed improved sensitivities (S=53.2nC/μM for Cefoperazone) and a good reproducibility around 97%. The response is linear in the Cefoperazone concentration range of 2 to 120×10^{-9} M with a detection limit of 1.20×10^{-11} M. Moreover, the proposed method exhibited high sensitivity, fast response time (less than 5 s) and long-term stability. The proposed method was successfully used in the determination of Cefoperazone content in the pharmaceutical formulation.

Keywords: FFT Coulometric Admittance Voltammetry; Carbon paste, Cefoperazone, CeO_2 nanoparticles; Graphene nanosheets; Au nanoparticle; ionic liquid

1. INTRODUCTION

Cefoperazone (Figure 1) is one of the most important third generation cephalosporin antibiotic with a board spectrum of activity against gram-positive and gram-negative bacteria and have activity against β-lactamases [1,2]. It is clinically effective in the treatment of infections in the biliary tract and the ideal drug for the treatment of biliary tract infection should have excellent effects against potential biliary pathogens and should easily penetrate and be concentrated in the biliary tree [3-5]. In veterinary

medicine, cephalosporins are widely used to treat and prevent various infectious diseases and this can be a potential risk because drug residues may be present in biological fluids and tissues. Thus, sensitive determination of cephalosporins in biological samples is required in various fields such as therapeutic drug monitoring and analytical and forensic toxicology.

Several analytical methods have been reported to determination of in Cefoperazone biological fluids, including spectrophotometric [6], high performance liquid chromatography (HPLC) [7], Square-wave voltammetric [8] and chemiluminescence detection [9].

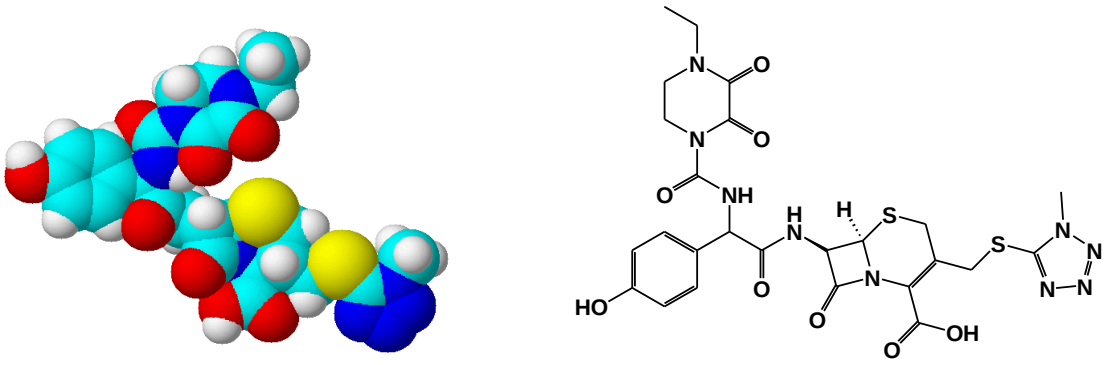

Figure 1. Chemical 3D and 2D structure of Cefoperazone.

In recent years, metal oxide nanoparticles such as ZnO, SnO_2, MnO_2, TiO_2 and CeO_2 have been used for fabrication of electrochemical sensor and biosensors [10-16]. Cerium oxide is considered as a perfect metal oxide for immobilization of organic molecules with oxygen groups.

It is well known that nanomaterials of carbon, like graphene nanosheets (GNS) demonstrate high surface area and excellent electrical conductivity in new designed electrodes, also, it helps to establish a larger number of active sites for adsorption of organic molecules [17,18]. Those excellent characterizations of GNS the high conductivity can facilitate the electron transfer of electroactive species. Moreover, in order to improve the performance of the carbon paste electrode, ionic liquids (IL) can be very helpful as a binder in the carbon pate electrodes [19,20]. Here, IL was used as a binder in the nanocomposite electrode to its high ionic conductivity, good stability and well biocompatibility.

In this work, a new nano-composite modified carbon paste electrode (MCPE) for Cefoperazone deterioration is presented. The new electrode was fabricated by mixture of 1-butyl-3-methylimidazolium hexafluorophosphate ($BMIMPF_6$), graphene nanosheets (GNS), CeO_2 and Au nanoparticles. Where, the electrode response was obtained by a special square wave electrochemical method called coulometric FFT admittance voltammetry (CFFTAV) [21-27]. The presence of GNS in the MCPE offers a significant enhancement in the analytical response. Under optimal conditions, the designed sensor exhibited a linear response to Cefoperazone concentrations. For determination of Cefoperazone, the admittance of the sensor was measured during the potential ramp and then the response in form of coulomb was calculated.

2. MATERIALS AND METHODS

2.1. Reagents

All chemicals and solvents used were of analytical grade and used as received without further purification. Double distilled water was used throughout the experiments. Cefoperazone was purchased from Sigma-Aldrich. Cefoperazone was stored in the frozen state, and its standard solutions were prepared daily with double distilled water when in use. The prepared solutions were kept at 4 °C before use.

Graphite powder with a 1–2 μm particle size and high-purity paraffin oil (Merck) were used for the construction of the carbon pastes. Cerium oxide nanoparticles (CeO_2 NPs, 99.9%, 10-30 nm) were purchased from local company in Iran. The graphene nanosheets thickness is about 7 nanometers, with an average surface area of about 120 to 150 m2/g was purchased from XG Sciences Co. Ionic liquid, 1-butyl-3-methylimidazolium hexafluorophosphate ($BMIMPF_6$) and other chemical used were all purchased from Merck Co.

2.2. Electrode Preparation and electrochemical Instrumentation

The traditional carbon paste electrode (CPE) was prepared by hand mixing and carefully grinding in an agate mortar 400mg of graphite powder, 0.5-6 mg of Au NPs and cerium oxide nano-powder, and 2-40 mg graphene nanosheets with IL as suitable binder.

A portion of the resulting homogeneous paste was packed firmly into a Teflon tube (3mm in diameter). Electrical contact was established through a copper wire to the end of the paste in the inner hole of the tube. The schematic diagram of the electrode was shown in Figure 2.

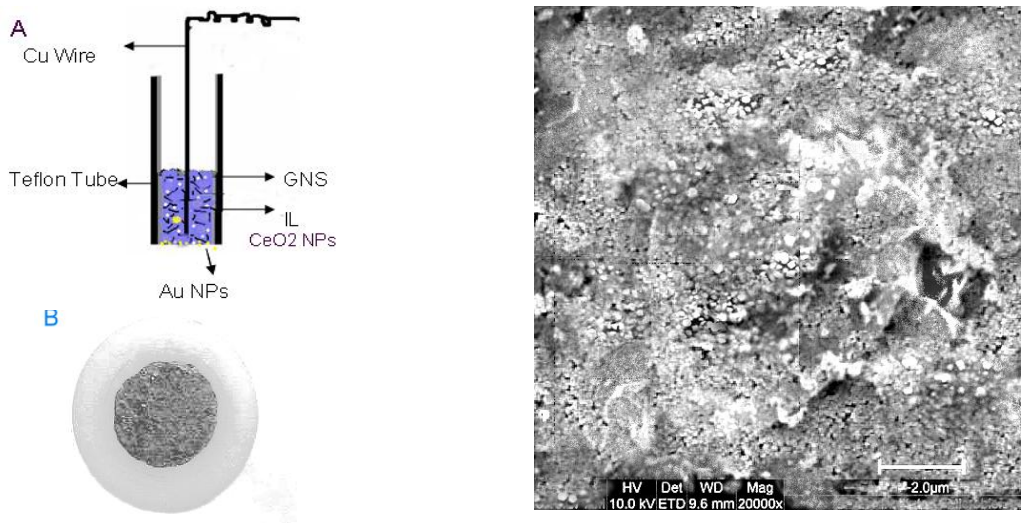

Figure 2. A) Schematic diagram of constructed MCPE, the Teflon tube filled with the paste and used for determination of Cefoperazone; and SEM images of MCPE surface.

The electrochemical CFFTAV measurements carried out with a homemade potentiostat. For controlling, it was connected to a PC equipped by an analog to digital data acquisition board (PCL-818H, Advantech Co.). During the measurements, the memory and CPU requirements of the computer were ordered or controlled by the electrochemical software that was developed in the lab.

A special square wave potential waveform was repeatedly applied to the working electrode and then the current data was acquired, and stored by the software. The electrochemical program was employed to generate an analog waveform and acquire admittance readings. It, also, processed and plotted the data in real time. In fact, coulometric signal of the MCPE was calculated by integrating of the net admittance changes is over the selected scanned potential range. In this method, ΔQ is calculated based on the admittance changes at the voltammograms in the integration potential range of the admittance. The sensor response (which is charge change under the peak) was calculated as ΔQ;

$$\Delta Q = Q - Q_0 \quad (1)$$

where Q is the electrical charge obtained by integration of admittance voltammetric curve between 200 and 900 mV , and Q_0 represents Q in the absence of the adsorbent. Moreover, the results indicate that with increasing the concentration of Cefoperazone in the injected sample, ΔQ increases proportionally.

3. RESULTS AND DISCUSSION

Figure 2 shows the cyclic voltammograms of 3.0 mM $[Fe(CN)_6]^{3-/4-}$ at two type of electrodes, CPE and MCPE. For the both electrode CPE, a couple of a smaller redox peaks could be observed in the potential from 700 V to –400 mV (curve a), which may be attributed to the weak electrical conductivity or low active sites of the normal CPE. On the other hand, for the peak currents at the MCPE (curve b) increased significantly in comparison with those of curve a.

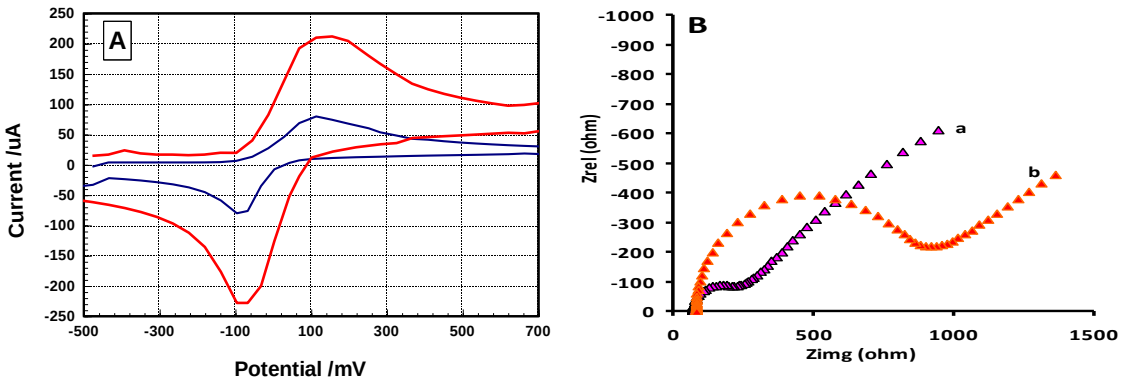

Figure 3. Cyclic voltammograms of 3.0 mM $[Fe(CN)6]^{3-/4-}$ at a) CPE, (b), MCPE, Scan rate: 300 mV/s ; Nyquist plots recorded at (a) bare MCPE, (b) CPE, Supporting electrolyte solution is 3.0 mM $[Fe(CN)6]^{3-/4-}$ containing 0.1 M KCl

One explanation, for the electroactive current enhancement could be that GNS and Au NPs providing a large specific surface area on the sensor surface for the redox reaction, which could accumulate much more $[Fe(CN)6]^{3-/4-}$ on MCPE. Moreover, this property combine with synergistically improved conductivity in the mixture of IL, could increase the current response. It seems that the nanomaterials could act as tiny conduction centers, which facilitated the transfer of electrons. The other reason may be attributed to two aspects GNS and Au NPs serving as nano-connectors between CeO_2 NPs. The obtained results using admittance voltammetry measurements are in agreement with the obtained results from EIS meaasurments.

Fig. 3B shows results of EIS measurements carried out on CPE and MCPE electrodes in the buffer solution containing 3 mM $[Fe(CN)6]3^{-/4-}$ containing 0.1 M KCl. it is assumed for the Randles circuit, the resistance to electron transfer and the diffusion impedance is parallel to the interfacial double layer capacitance. In this figure, the semicircle portion, observed at higher frequencies, corresponds to electron-transfer-limited process, whereas the linear part is characteristic of the lower frequencies range and represents the diffusion-limited electron-transfer process. It can be seen that semicircle diameter of CPE is larger than that of MCPE, indicating higher electron transfer resistance at the electrode interface.

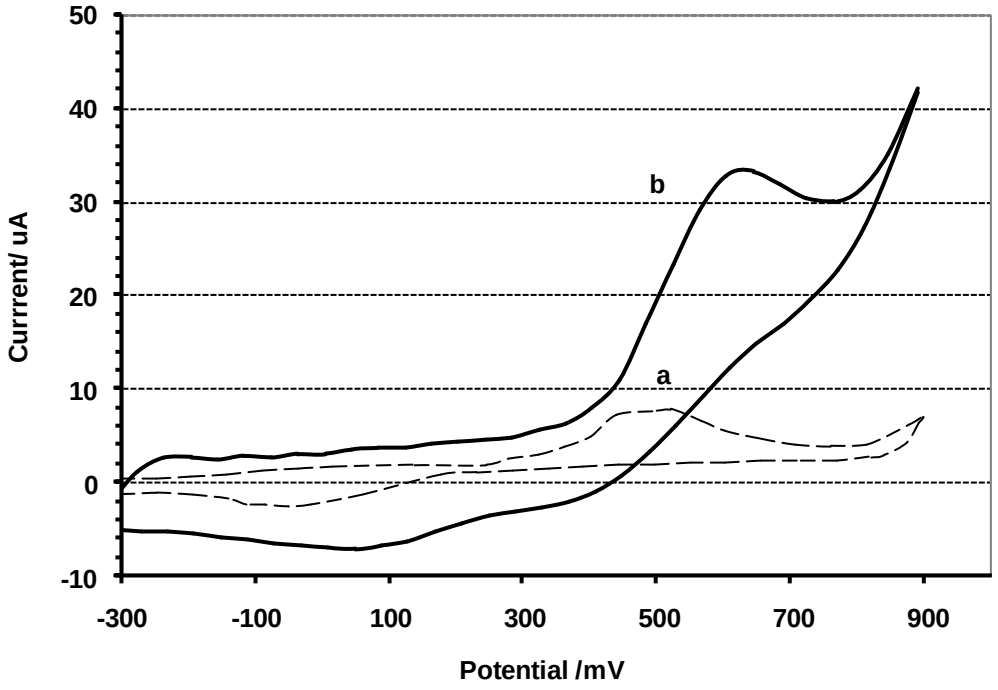

Figure 4. Cyclic voltammograms of 1µM Cefoperazone in buffer on; (a) the unmodified CPE, and (b) MCPE; scan rate 300 mV/s

Fig. 4 showed the cyclic voltammograms of Cefoperazone on CPE (curve a) and MCPE (curve b) 0.05 M phosphate buffer solution at pH 4.0. Cefoperazone shows very weak redox peaks, at the bare CPE, this is an indication of the lower rate kinetic reaction of Cefoperazone on the CPE surface. On the other hand, for MCPE shows anodic peak at about 680 mV on the modified electrode, This

indicates that MCPE surface can enhance the electron-transfer rate and make more Cefoperazone participate in the electrochemical reaction due to their accumulation and catalytic ability.

3.1. Determination method

Fig. 5 shows CFFTAV and the changes in voltammetric of the MCPE sensor in the potential range of -200 to 1000 mV. The potential axis on this graph represents potential applied to the working electrode during each potential scan. The time axis represents the time passing of the experiment and the sweep number) [27-34]. The figure shows that at the begging of the experiment there is not an significance signal in the voltammograms, but after addition of 1.0×10^{-6} M Cefoperazone in the buffer solution at pH 4.5 a peak appears at potential 680 mV. The increase in the admittance at this potential could be due to the redox of Cefoperazone at the MCPE surface.

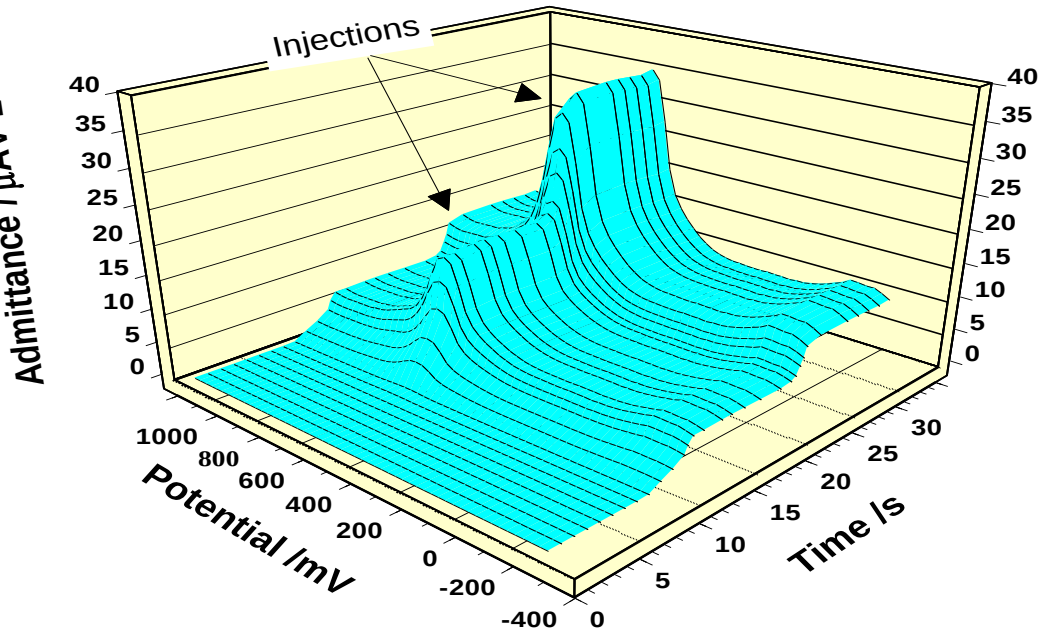

Figure 5. a) FFT admittance voltammograms of the MCPE sensor in absent and with addition of 1.0×10^{-6} M Cefoperazone in the buffer solution at pH 4.0. The square wave frequency was 700 Hz at amplitude 30 mV. Integration potential range for the admittance is 200 to 900 mV.

However, as mentioned above the accumulation of the Cefoperazone to high surface area of MCPE can enhance of direct electron transfer between the active sites of the biosensor. This can increase the peak admittance at the recorded voltammograms, when the sample was added to calculate the sensor response in form of ΔQ based on equation 1, the integration range was from 200 to 900 mV.

The unit for value of the sensor response for Cefoperazone, sample suction after calculation is in coulomb (C).

3.2. Optimization of SW frequency and amplitude

Due to this fact that, in CFFTAV method the admittance voltammetric response of the sensor depends on the applied conditions of excitation waveform, it was needed to study the influence of the square wave frequency and amplitude on the analyte response. To obtain the optimum square wave condition in for maximum value of ΔQ, the measurements was carried out at the square wave frequency range 100-1400 Hz and amplitude 5 to 50 mV.

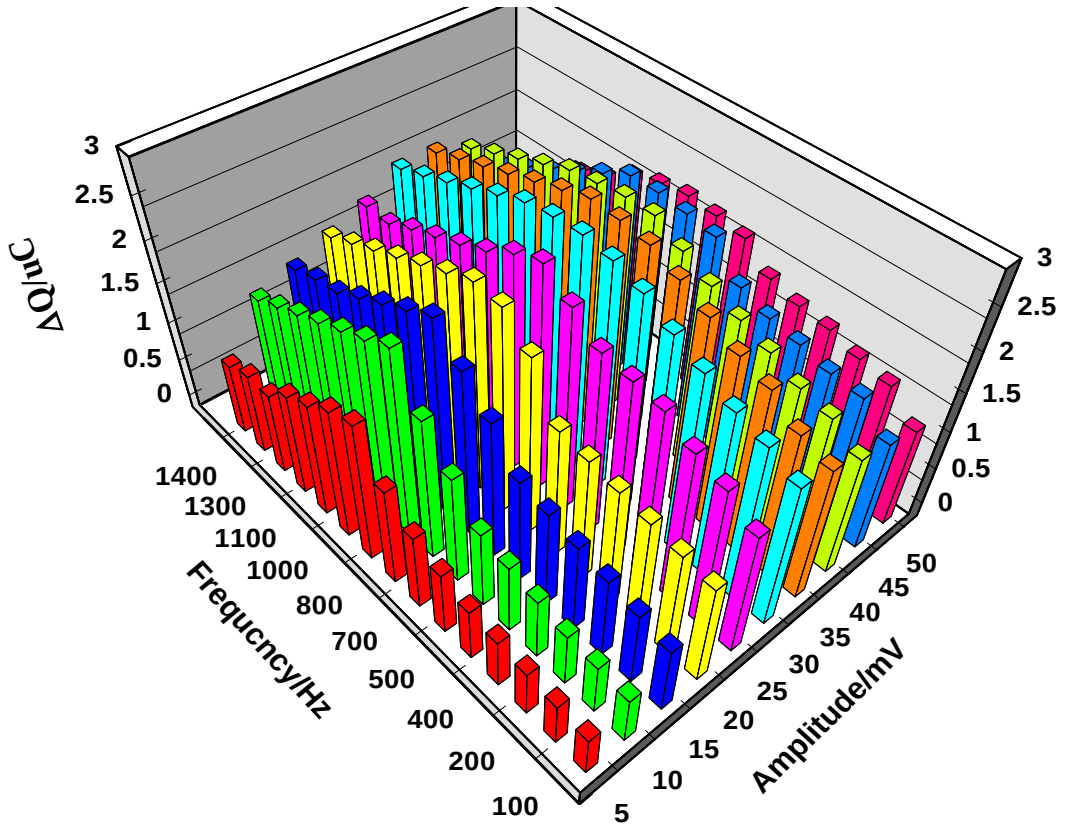

Figure 6. The effect of frequency and amplitude on the response of MCPE sensor to addition of 1.0×10^{-6} M Cefoperazone in the buffer solution at pH 4.0.. Integration potential range for the admittance is 200 to 900 mV.

In Fig. 6 the results of change in the response at various value of the square wave frequency and amplitude is demonstrated for solution of 1 μM of Cefoperazone at pH 4.0. It is well know that the value of a signal for the oxidation processes noticeably effected by changing the applied square wave frequency. This dependency can be realized in the graph, in which the sensor response increases with SW frequency up to 700 Hz. Such enhancement can be seen for the amplitude up to 30 mV. The

enhancement of the signal may due to improvement is similar to the enlargement of current in cyclic voltammetry with potential scan rate. However, after that value the signal decline. This may due to kinetic limitation in electron transfer rate. Furthermore, the background noise and peak shape of Cefoperazone are depends on the factors in the applied potential waveform. Therefore, it is expected that the value of the sensor response is limited at high values of the square wave frequency and amplitudes.

3.3. Optimization of pH and the sensor composition

The dependence of the MCPE response to Cefoperazone solution in various pH values was investigated. Fig.7 shows the change in response of the sensor for addition of 1.0×10^{-6} M Cefoperazone in the buffer solution at pHs 2 to 8. The following measurements were recorded at frequency 700 Hz and amplitude 20 mV.

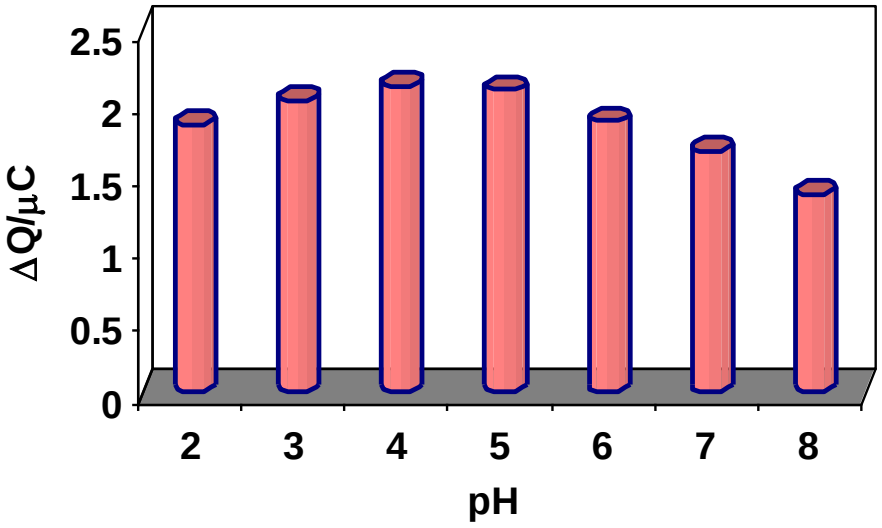

Figure 7. The effect of pH on the response of MCPE sensor to addition of 1.0×10^{-6} M Cefoperazone in the buffer solution. The square wave frequency was 700 Hz at amplitude 30 mV. Integration potential range for the admittance is 200 to 900 mV.

The results showed that when pH of the buffer solution was increased up to 4, oxidation admittance peak improved and oxidation potential shift to less positive potential. This is an induction of facilitated electron transfer at the senor surface. Conversely, at pHs higher than 4, the magnitude of the MCPE response decreased. Therefore, pH 4 was selected as the optimal pH for detection in the following experiments.

As mentioned above, the existence of nanoparticles in the composition of the MCPE can enhance the catalytic properties of the sensor. However, such propertie depend on the quantity of the nanoparticles used in fabrication of the sensor. Therefore, weight of CeO_2 NPs and GNS in the

composition of MCPE was investigated. Fig.7 shows the obtained results of CFFTAV measurements solution of 2 μM Cefoperazone with MCPE.

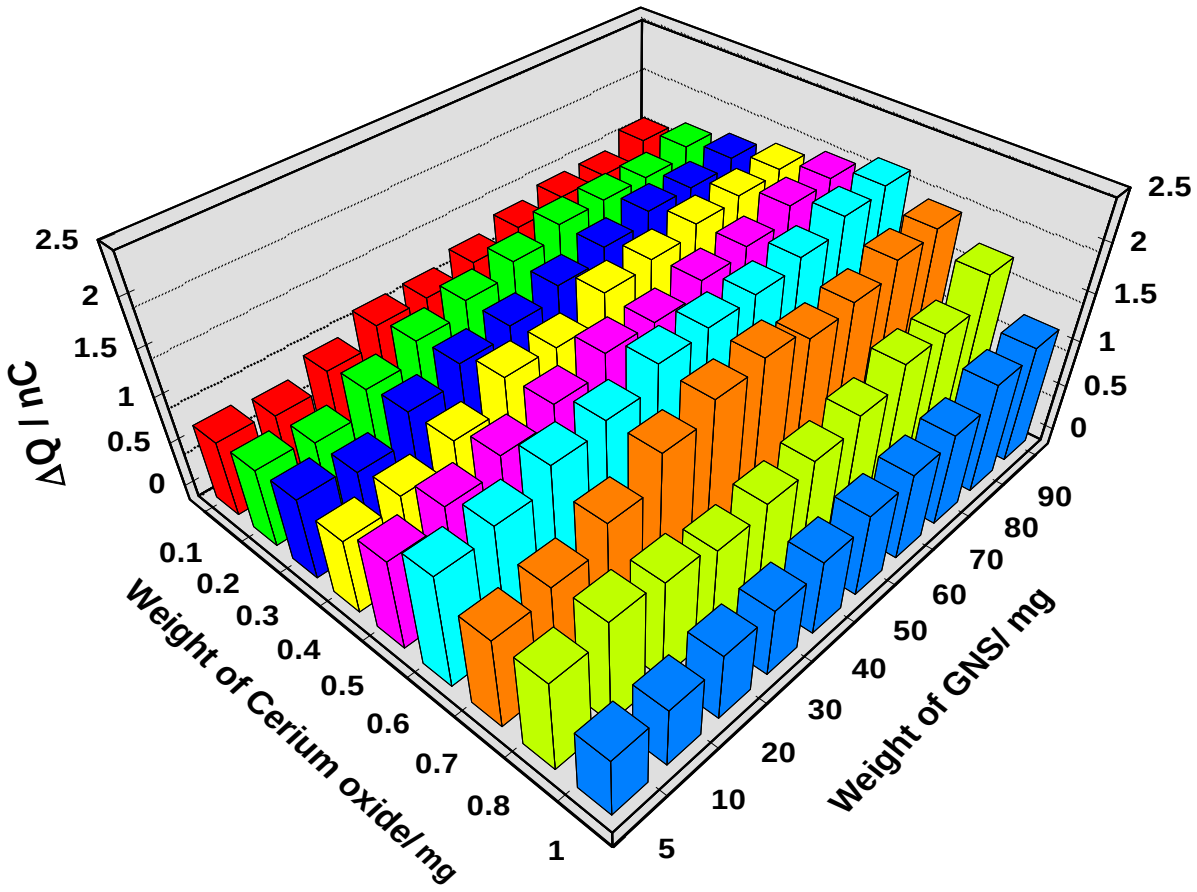

Figure 8. The effect of weight of NPs on the response of MCPE sensor to addition of 1.0×10^{-6} M Cefoperazone in the buffer solution at pH 4.0. The square wave frequency was 700 Hz at amplitude 30 mV. Integration potential range for the admittance is 200 to 900 mV.

The composition of MCPE contains various weights of GNS, in range of 10-60 mg, and various weights of CeO_2 NPs, in range of 0.1-1 mg. These data indicate that the optimum weight of is GNS 40 mg, and the optimum weight of CeO_2 NPs is 0.6 mg. It can be suggest that at up to the maximum weight of NPs, the oxidation process of the analyte advanced. However, after the optimum value, the excess weight of CeO_2 may inhibit the reaction of Cefoperazone with the electrode. It may due to development the distances between the adsorbed analyte and the other conductive NP, which are responsible for electron transfer. Consequently, the sensor response reduces after the maximum value. In case of GNS, at first, it can be seen that a raise in the sensor response with increasing of weight of GNS up to 60 mg, while after the optimum value, the sensor response decline. It means that GNS can help the sensor sensitivity via increasing surface contact with Cefoperazone.

3.4. Calibration curve and biosensor characterization

In this electrochemical detection method, the differential integrated admittance peak area of Cefoperazone (referred to as ΔQ as shown in equation 1), was used for plotting the calibration curve.Fig. 8A illustrates a typical ΔQ response of MCPE for addition of standard solutions of Cefoperazone, where the experimental parameters were set at optimum values of factors, in order to obtain the best detection limits for the sensor.

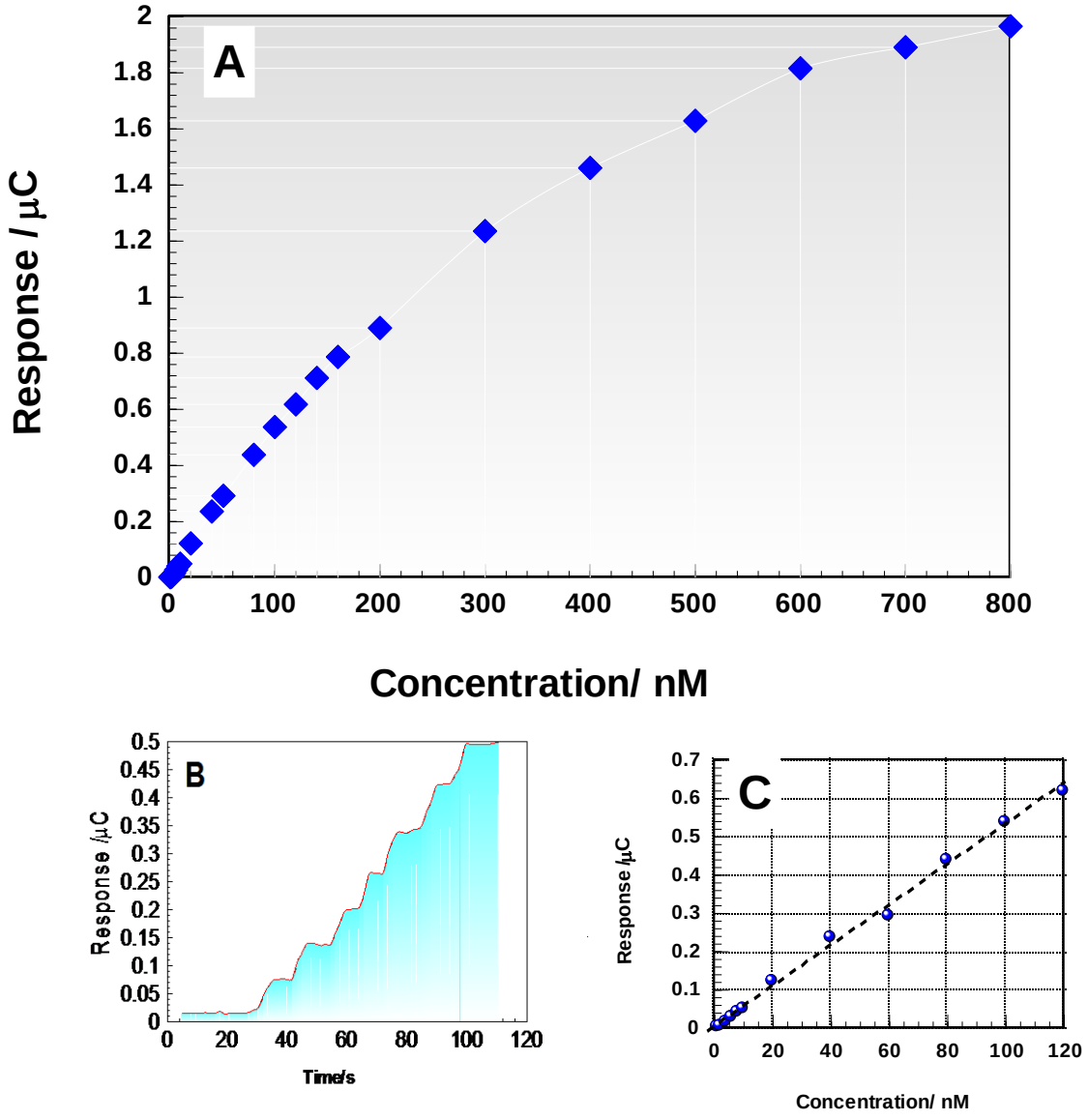

Figure 9. A) The calibration curve for Cefoperazone standard solutions in pH 4.0. B) Response of the MCPE to upon the following addition of 8 nM of Cefoperazone solutions. C) The linear part of calibration curve for Cefoperazone standard solutions. Results shown in this figure represent the integrated signal for 3 consecutive additions of the Cefoperazone standard solution.

As can be seen in Fig. 8A, the ΔQ of Cefoperazone solutions (from 2.0 to 800.0 nM in PB, pH4.0) increased gradually with increments of the concentration of the analyte and lastly leveled off to

a more or less with a smaller slope. To obtain defection limit of the sensor for measurement of Cefoperazone, at first, a stock solution of 5 nM Cefoperazone was freshly prepared, and then for making the other standard solutions, an aliquot was diluted to the appropriate concentration (see Fig. 8B). Before each measurement, the three-electrode system was installed in a blank solution, and the admittance voltammetry scan from −200 to 1000 mV. Fig. 8C, shows the linear section of the curve (at low the concentrations from 2×10^{-10} to 120.0×10^{-9} M), and the calibration equation of the best-fitted line was y (μC)= 0.0053x(nM) + 0.0027 with a correlation coefficient of 0.997 (n = 5, SD = 0.0062). A detection limit of 1.20×10^{-11} M, three times the standard deviation of the blank solution, was estimated.

In these measurements, the obtained recoveries for the spike milk samples were ranged from 99.5% to 102.1% and the contents of Cefoperazone found are in good agreement with that specified by the manufacturers.

Table 1. Determination of Cefoperazone in pharmaceutical tablets by standard addition method (concentration in nM)

Samples	Detected	Added	Found	Recovery (%)
1	6.2	6.0	12.2	99.5
2	10.5	20.0	30.9	102.1
3	43.5	40.0	82.5	99.3
4	43.9	40.0	83.9	101.3

Table 2. The comparison of the determination of Cefoperazone with nano-composite carbon paste electrode with the previous reported methods based on the utilization of different materials and techniques

Ref.	Detection Method	DL	Electrode & Materials
[35]	Square wave voltammetric	0.375 ng ml^{-1}	Hanging mercury drop electrode (HMDE)
[36]	Square-wave voltammetry (SWV)	0.5 nmol L^{-1}	Hanging mercury drop electrode (HMDE)
[37]	Flow injection chemiluminescence	0.06 μg ml^{-1}	Permanganate, presence of perchloric acid, catalysed by Mn(II)
This work	Admittance FFCV	0.077 ng ml^{-1}	MCPE by IL, grapheme nanosheet, Au and CeO_2 NPs

The results are shown in Table 1. These results indicate that the CFFTA voltammetry method has acceptable precession and accuracy for rapid and sensitive determination of Cefoperazone in

pharmaceutical tablets. Also, in evaluation, the performances of the fabricated biosensor is compared with some of the best previously reported Cefoperazone sensors based on the utilization of different materials as the working electrode and different detection techniques (Table 2) and it was confirmed that the presented NPs and based Cefoperazone sensor with CFFTAV exhibited an excellent and reproducible sensitivity.

3.5. Stability and reproducibility of the Electrode

The sensor was evaluated by examining the analyte response, using CFFTAV method over a long time period. The sensor storage stability was investigated for 60 days at room temperature when not in used. The results showed that the sensitivity reduce only 4.4± 0.2% up that time, which gradually decreases afterwards might be due to the adsorption of impurities. In addition, after that time the sensor response reaches to 95.6± 0.3% of the initial current response was retained, indicating that sensor was fairly stable and good reproducibility.

4. CONCLUSIONS

A new determination method has been developed for the detection of Cefoperazone in real samples based on CFFTAV response and nano-composite modified carbon paste electrode. Nano-composite paste was made by mixing ionic liquid, 1-butyl-3-methylimidazolium hexafluorophosphate ($BMIMPF_6$), graphene nanosheets, Au and CeO_2 nanoparticles as electrochemical mediators. The assay provides a much improved sensitivity for the detection of Cefoperazone. Thus, the graphene nanosheets, Au and CeO_2 nanoparticles provided a novel means of constructing an electrochemical MCP sensor. Under optimal conditions, the designed sensor exhibited a wide linear response to Cefoperazone concentration, good sensitivity, a fast response time, repeatability and long term stability, 60 days with a decrease of 4.4±0.2% in response. Future experiments will be required to study the various factors in detail so as to lessen the influence of the environment, and investigate its application to CFFTAV detection.

ACKNOWLEDGEMENT
The authors are grateful to the Research Council of University of Tehran for the financial support of this work.

References

1. S.L. Barriere, and J.F. Flaherty, *Clin. Pharm.* 3 (1984) 351.
2. W.A. Craig, and A.U. Gerber, *Drugs* 22 (1981) 35.
3. M.G. Bergeron, J. Mendelson, G.K. Harding, L. Mandell, I.W. Fong, A. Rachlis, R. Chan, S. Biron, R. Feld, and N.B. Segal, *Antimicrob. Agent Chemother.* 32 (1988) 1231.
4. J.S. Dooley, J.M. Hamilton-Miller, W. Brumfitt, and S. Sherlock, *Gut* 25 (1984) 988.
5. J.V. Hirschmann, and T.S. Inui, *Infect. Dis.* 2 (1980) 1.

6. A. Parra, J. Garcia-Villanova, V. Rodenas, and M.D. Gomez, *J. Pharm. Biomed. Anal.* 12 (1994) 653.
7. T.L. Tsou, Y.C. Huang, C.W. Lee, A.R. Lee, H.J. Wang, and S.H. Chen, *J. Separat. Sci.* 30 (2007) 2407.
8. S. Billová, R. Kizek, F. Jelen, and P. Novotná, *Anal. Bioanal. Chem.* 377 (2003) 362.
9. F. Li, M. Qiao, and X. Guo, *Biomed. Chromatogr.* 17 (2003) 53.
10. W. Zhang, X. Zheng and K. Jiao, *Sens. and Actuators B* 162 (2012) 396.
11. Z. F. Deng, H. W. Zhang and Y. Z. Jiao, *Chinese J. Anal. Chem.* 37 (2009) 613.
12. X. Q. Hou, X. L. Ren, F. Q. Tang, D. Chen and Z. P. Wang, *Chinese J. Anal. Chem.* 34 (2006) 303.
13. P. Norouzi, F. Faridbod, E. Nasli-Esfahani, B. Larijani and M. R. Ganjali, *Int. J. Electrochem. Sci.* 5 (2010) 1008.
14. J. J. Xu, W. Zhao, X. L. Luo and H. Y. Chen, *Chem. Commun.* 6 (2005) 792.
15. H. M. Cao, Y. H. Zhu, L. H. Tang, X. L. Yang and C. Z. Li, *Electroanalysis* 20 (2008) 2223.
16. K. J. Feng, Y. H. Yang, Z. J. Wang, J. H. Jiang, G. L. Shen and R. Q. Yu, *Talanta* 70 (2006) 561.
17. A. H. Castro Neto, F. Guinea, N. M. R. Peres, K. S. Novoselov and A. K. Geim, *Rev. Mod. Phys.* 81 (2009) 109.
18. C. Soldano, A. Mahmood, and E. Dujardin, *Carbon*, 48 (2010) 2127.
19. F. Faridbod, M. R. Ganjali, M. Pirali-Hamedani and P. Norouzi, *Int. J. Electrochem. Sci.*, 5 (2010) 1103.
20. M. R. Ganjali, H. Khoshsafar, A. Shirzadmehr, M. Javanbakht and F. Faridbod, *Int. J. Electrochem. Sci.*, 4 (2009) 435.
21. P. Norouzi, H. Rashedi, T. Mirzaei Garakani, R. Mirshafian and M. R. Ganjali, *Int. J. Electrochem. Sci.* 5 (2010) 377.
22. P. Norouzi, M. R. Ganjali, B. Larijani, A. Mirabi-Semnakolaii, F. S. Mirnaghi, and A. Mohammadi, *Pharmazie* 63 (2008) 633.
23. P. Norouzi, M. R. Ganjali, S. Shirvani-Arani, and A. Mohammadi, *J. Pharm. Sci.* 95 (2007) 893.
24. M. R. Pourjavid, P. Norouzi, and M. R. Ganjali, *Int. J. Electrochem. Sci.* 4 (2009) 923.
25. P. Norouzi, M. R. Ganjali, M. Zare, and A. Mohammadi, *J. Pharm. Sci.* 96 (2007) 2009.
26. P. Norouzi, M. Qomi, A. Nemati, and M. R. Ganjali, *Int. J. Electrochem Sci*. 4 (2009) 1248.
27. P. Norouzi, B. Larijani, M. Ezoddin and M. R. Ganjali, *Mater. Sci. Eng. C* 28 (2008) 87.
28. M. R. Ganjali, P. Norouzi, R. Dinarvand, R. Farrokhi, and A. A. Moosavi-Movahedi, *Mater. Sci. Eng. C* 28 (2008) 1311.
29. P. Norouzi, M. R. Ganjali, and L. Hajiaghababaei, *Anal. Lett*., 39 (2006) 1941.
30. P. Norouzi, G. R. Nabi Bidhendi, M.R. Ganjali, A. Sepehri, M. Ghorbani, *Microchim. Acta*, 152 (2005) 123.
31. M. R. Ganjali, P. Norouzi, M. Ghorbani, and A. Sepehri, *Talanta*, 66 (2005) 1225.
32. P. Norouzi, H. Ganjali, B. Larijani, F. Faridod, M. R. Ganjali, and H. A. Zamani, *Int. J. Electrochem. Sci.* 6 (2011) 5189.
33. P. Norouzi, B. Larijani, F. Faridod, M. R. Ganjali, *Int. J. Electrochem. Sci.* 5 (2010) 1550.
34. P. Norouzi, M. R. Ganjali, M. Qomi, A. N. Kharat, H. A. Zamani, *Chinese J Chem.*, 28 (2010) 1133.
35. E. Hammam, M.A. El-Attar, A.M. Beltagi, *J. Pharm. Biomed. Anal.* 42 (2006) 523-527.
36. Sabina Billová, René Kizek, František Jelen, Pavla Novotná, *Anal. Bioanal. Chem.* 377 (2003) 362.
37. C. Thongpoon, B. Liawruangrath, S. Liawruangrath, A. Wheatley, A. Townshend, *Anal. Chim. Acta* 553 (2005) 123.